TEORIJSKA I PRIMENJENA MEHANIKA 15, pp 55–66, 1989, UDK 621.78.019.8

SHORT CRACK THRESHOLD STRESS INTENSITIES AND DEFECT TOLERANCE OF 52100 BEARING STEEL

Aida Kadić, Hajrudin Pašić

(Received 24.05.1989; revised 14.07.1989)

This work contains results of investigations on short crack threshold stress intensities and defect tolerance of SAE 52100 bearing steel. An analytical model for short crack propagation prediction is developed. This model is based on elastic-plastic fracture mechanias approach and the effective stress intensity (and closure) concept. The threshold effective stress intensity values are compared with those from the only existing, Newman's, analytical model. These values have been used to make defect tolerance and crack propagation modes predictions based on the Tanaka resistance curve approach.

1. Introduction. Fatigue crack propagation in engineering materials has been the subject of considerable research. Most of the investigations focused on the behavior of long fatigue cracks, even though the characteristics associated with the extension of small cracks in metals and alloys remain relatively unexplored, despite their unquestionable importance from an engineering standpoint.

Cracks are defined as being short [1, 2, 3]:

(i) when their length is short compared to relevant microstructure dimension (a continuum mechanics limitation),

(ii) when their length is compared to the scale of local plasticity (LEFM limitations) or,

(iii) when they are simply physically small (e.g. < 0.5–1 mm)

Since all three types of short flaw are known to propagate faster than (or at least at the same rate as) corresponding long fatique cracks subjected to the same nominal driving force, current defect tolerant fatigue design procedures which utilize long crack data can, in certain applications, result in overestimate of lifetimes.

Results obtained by Lankford [4,5], Taylor and Knott [6] and others [2] have shown that there is generally a variation between growth rates for long (solid line) and short (dashed lines) cracks, Fig. 1.

The growth rates for the short cracks are up to two orders of magnitude faster than those of the long cracks, and such accelerated short crack advance occurs at stress intensity ranges well below the long crack fatigue threshold stress intensity

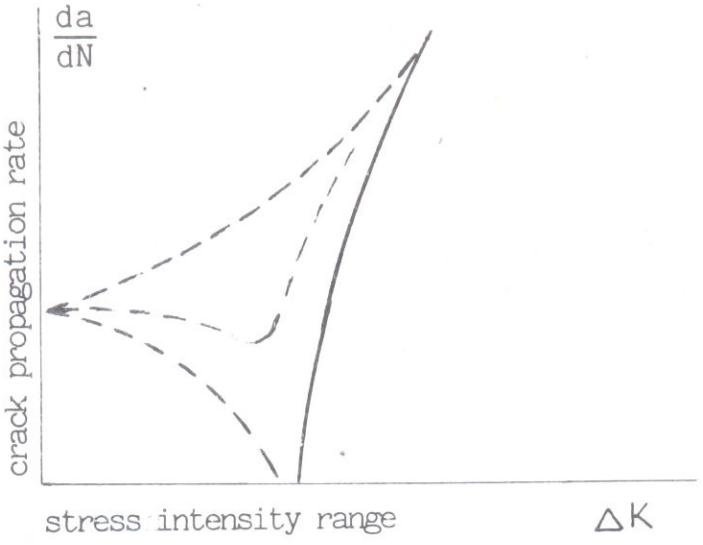

Figure 1

range ($\Delta K_{th\infty}$). The initially higher growth rates of a short crack decelerate progressively (and even arrest in certain cases) before merging with the long crack data at stress intensities close to $\Delta K_{th\infty}$ [3,4,5,6]. The behavior of short cracks has been rationalized in terms of the deceleration of growth as a result of crack closure and through interactions with microstructural features, particularly grain boundanies in soft variants [2,5].

From experimental studies, it is apparent that threshold stress intensities associated with long and short cracks are different. Conventional fracture mechanics arguments imply that the threshold stress intensity range (ΔK_{th}) for particular material should be independent of crack length (i.e. $\Delta K_{th\infty}$, the long crack threshold, is constant). Kitagawa and Takahashi [7], however, first showed that below a critical crack size a_0 the threshold for short cracks ΔK_{th} decreased with decreasing crack length, while the threshold stress σ_{th} approached endurace limit σ_e. Critical crack size (below which ΔK_{th} is no longer constant with crack size) depends on microstructural and mechanical factors.

El Haddad et al. [8] have proposed an empirical approach based on the notion of an intrinsic crack length parameter a_0. They redefined the stress intensity factor K in terms of the physical crack length a plus a_0, so that the stress intensity range ΔK which characterizes the growth of fatigue cracks is given by the equation

$$\Delta K = 1.12\Delta\sigma\big(\pi(a + a_0)\big)^{1/2},$$

where stress is denoted by σ. The critical crack length a_0 is estimated from limiting condition

$$a \to 0 \qquad \Delta\sigma = \Delta\sigma_e, \quad \Delta K = \Delta K_{th},$$

where σ_e is endurance limit defined as a fatigue strength at 5×10^6 cycles, and ΔK_{th} is threshold value of stress intensity factor for long cracks. Therefore

$$a_0 = (1/\pi)\big(\Delta K_{th\infty}/1.12\Delta\sigma_e\big)^2. \tag{1}$$

The value of the intrinsic crack size a_0 is the critical crack size above which ΔK_{th} becomes constant equal to the long crack threshold stress intensity $\Delta K_{th\infty}$. In

other words, a_0 is an indication of the smallest crack size that can be characterized at the threshold in terms of LEFM. However, elastic-plastic fracture mechanics (EPFM) gives better estimate of critical crack size including closure effect.

Elber [9,10] first showed that interference and physical contact between mating fracture surfaces in the wake of crack tip can, under positive loads during the fatigue cycle, lead to effective closure of the crack. Since the crack cannot propagate while it remains closed, the net effect of closure is to reduce the nominal stress intensity range $\Delta K = K_{max} - K_{min}$ to some lower effective value ΔK_{eff} actually experienced at the crack tip, i.e. $\Delta K_{eff} = K_{max} - K_{op}$ where K_{op} is the stress intensity at opening (closure). If the scale of crack tip plasticity and microstructure are small with respect to the crack length, ΔK_{eff} is expected to provide correlation of short and long crack data [2]. The mechanisms of crack closure are illustrated schematically in Fig. 2 [11]. The closure effect occurs due to plasticity, surface roughness, residual stresses and oxide debris.

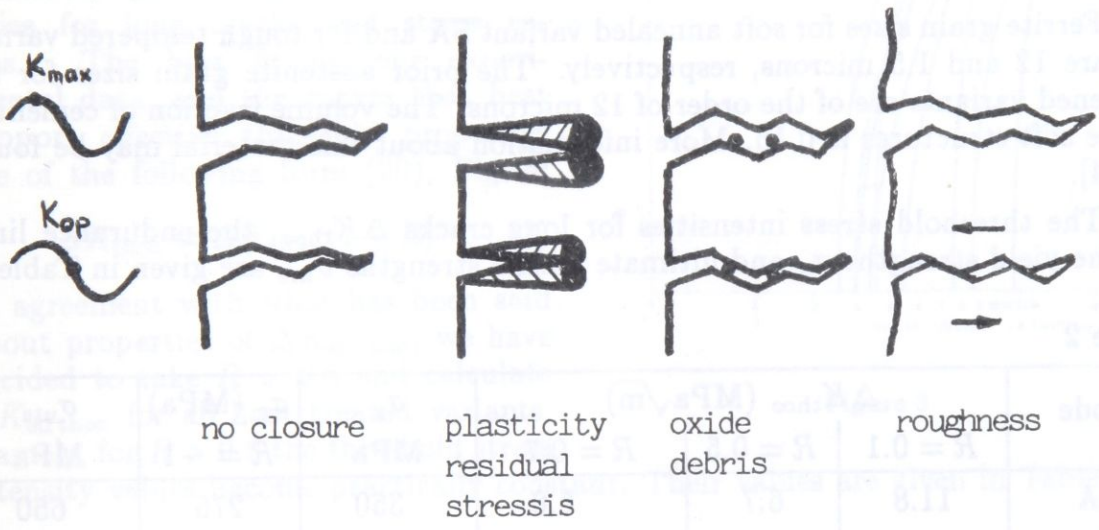

Figure 2

Tanaka et al. [12,13] proposed the use of threshold effective stress intensity $\Delta K_{eff\,th\infty}$ instead of $\Delta K_{th\infty}$ in Kitagawa-Takahashi diagram. They estimated new value for critical crack length

$$a_0' = (1/\pi)(\Delta K_{eff\,th\infty}/1.12\Delta\sigma_e)^2 \qquad (2)$$

and following the idea of El Haddad et al. obtained, what is called, a resistance curve which gives more conservative estimate than the one El Haddad had. For the cracks longer than a_0', $\Delta K_{eff\,th}$ becomes a constant independent of crack length, equal to threshold effective stress intensity for long cracks $\Delta K_{eff\,th\infty}$.

The present work is based on a Tanaka and Nakai approach using effective stress intensities. We made an estimate of $\Delta K_{eff\,th\infty}$ through analysis of long crack data for $\Delta K_{th\infty}$ rather than by measurement of K_{op} in 52100 bearing steel in various heat treated conditions. The critical crack length a_0' is then calculated based on experimental data for given steel and different heat treatments.

2. Materials and Mechanical Properties. The chemical composition of SAE 52100 is 1 C, 0.25 Si, 0.35 Mn, 1.5 Cr. The heat treatment codes for through-hardening bearing steels are in Table 1.

Table 1

code	Austenization			Quenching			Tempering		
	Furnace	Temp.	Time	Med.	Temp.	Time	Furn.	Temp.	Time
N	salt bath	860°C	20 min	oil	50°C	15 min	air cir.	160°C	90 min
B	salt bath	860°C	20 min	salt	235°C	5 hrs	—	—	—
S1	salt bath	860°C	20 min	salt	160°C	3 min	air cir.	240°C	4 hrs
MA	salt bath	830°C	20 min	salt	160°C	3 min	air cir.	240°C	4 hrs

Ferrite grain sizes for soft annealed variant SA and for tough tempered variant TT are 12 and 1.5 microns, respectively. The prior austenite grain sizes for the hardened variants are of the order of 12 microns. The volume fraction of cementite in the soft structures is 0.15. More information about this material may be found in [14].

The threshold stress intensities for long cracks $\Delta K_{th\infty}$, the endurance limit σ_e, the yield strengths σ_y and ultimate tensile strengths σ_{uts} are given in Table 2.

Table 2

code	$\Delta K_{th\infty}$ (MPa$\sqrt{m}$)			σ_y	σ_e (MPa)	σ_{uts}
	$R = 0.1$	$R = 0.5$	$R = 0.7$	MPa	$R = -1$	MPa
SA	11.8	6.7	5.0	350	275	650
TT	8.6	4.9	—	570	335	690
N	4.0	3.6	3.4	1320	927	1700
B	7.8	4.6	—	2130	795	2335
S1	5.4	3.9	—	2170	—	2195
MA	4.4	3.7	—	2110	—	2345

Through the experimentally obtained points visual fit curves of long crack propagation rate versus stress intensity are drawn in Fig. 3 for various heat treatments for stress ratios $R = \sigma_{min}/\sigma_{max}$ equal to 0.1 and 0.5.

3. Theoretical Results and Discussion. The theoretical approach is based on ability to assess or measure threshold effective stress intensity for long cracks. Since we do not have experimental data for K_{op}, and therefore for the threshold effective stress intensity, an attempt was made to estimate this value using data available for threshold stress intensity for long cracks. Threshold values of $\Delta K_{eff\infty}$ for many steels have been found to lie generally in the range 2–3.5 MPam$^{1/2}$. Such values may then represent an intrinsic material property [16-19], which is a function

of the composition and microstructure. A reduction in the measured $\Delta K_{th\infty}$ for long cracks is observed as the load ratio R is increased. At high R values ($R > 0.6$) there is minimal effect of closure on the near-threshold crack growth rate. An intrinsic material threshold may be defined as the measured $\Delta K_{th\infty}$ at high load ratio, which is equal to the effective stress intensity range $\Delta K_{eff\,th\infty}$ at threshold for all load ratios, that is, R-independent.

The attempt to estimate $\Delta K_{eff\,th\infty}$ is now made by using a relation that correlates the threshold stress intensities for long cracks and stress ratios. The best fit for our experimental data, and the curves that best support effective threshold properties are of the following form (20), Fig. 4:

$$\Delta K_{th\infty} = \Delta K_{th0}/(1+R)^{\gamma}. \quad (3)$$

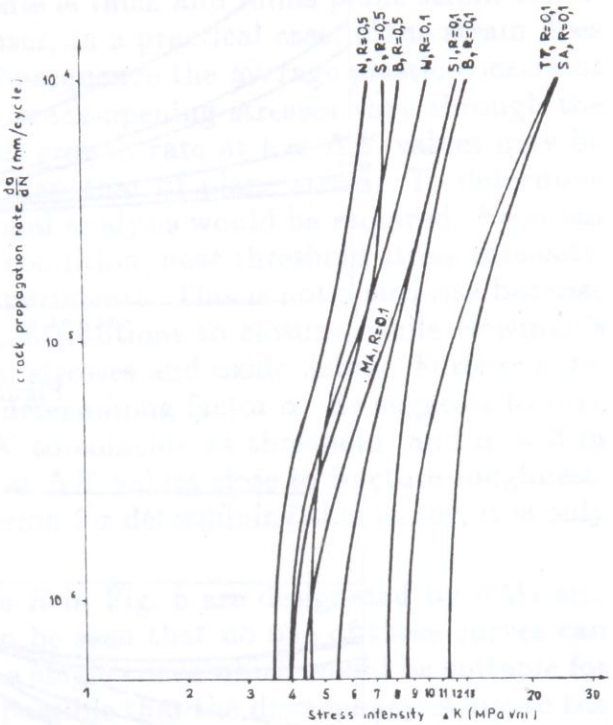

Figure 3

In agreement with what has been said about properties of $\Delta K_{eff\,th\infty}$, we have decided to take $R = 0.8$ and calculate $\Delta K_{eff\,th\infty}$ for all heat treated variants. Namely, for $R > 0.8$ the threshold stress intensity values become practically constant. Their values are given in Table 3.

Table 3

	SA	TT	N	B	S1	MA
$\Delta K_{eff\,th\infty}$	4.7	3.5	3.3	3.4	3.2	3.4

The theoretical approach to critical crack length can proceed with calculated values for $\Delta K_{eff\,th\infty}$. Since

$$\Delta K_{eff\,th\infty} = (K_{max} - K_{op})_{th\infty} = \left(1 - (K_{op}/K_{max})_{th\infty}\right)\Delta K_{th\infty}/(1-R),$$

there follows

$$(K_{op}/K_{max})_{th\infty} = 1 - (1-R)\Delta K_{eff\,th\infty}/\Delta K_{th\infty}.$$

Fig. 5 illustrates dependency of $(K_{op}/K_{max})_{th\infty}$ on R. For $R > 0.8$ all curves asymptotically approach straight line $(K_{op}/K_{max})_{th\infty} = R$. In this figure curves obtained by using Newman's model [21,22], which will be briefly discussed, are also given.

Newman's analytical expression for $(K_{op}/K_{max})_{th\infty}$ is obtained by finite element method, using two-dimensional, isotropic, homogenous, plane strain and

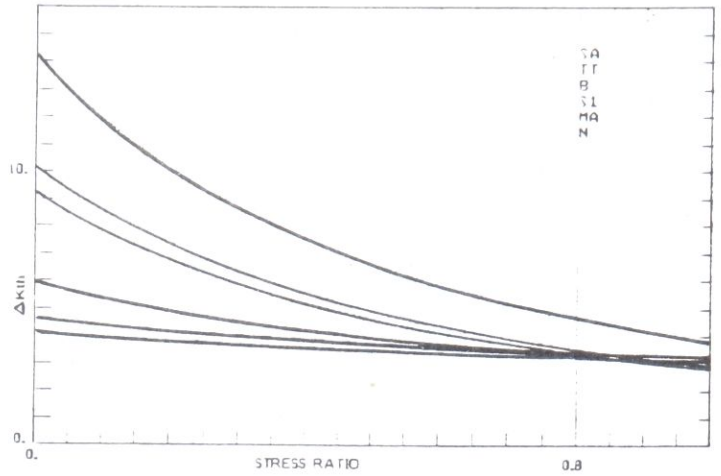

Figure 4

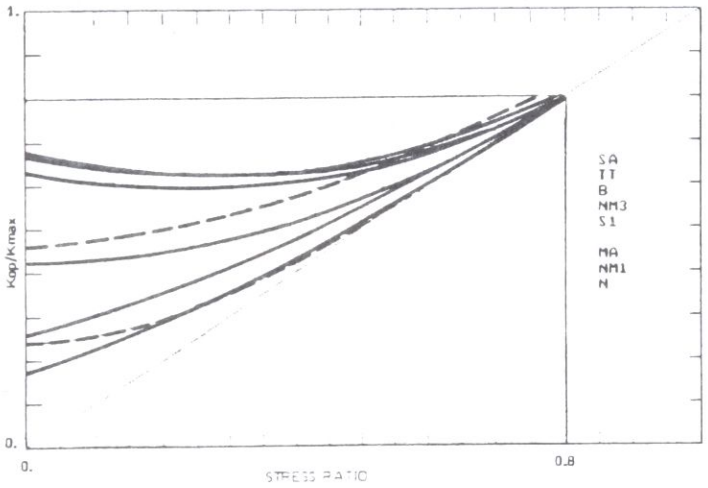

Figure 5

plane stress model with rigid ideally plastic constitutive relations [22,23]. He analyses only plasticity induced closure, disregarding closure due to surface roughness, residual stresses and oxide debris. That analytical expression is [21]:

$$(K_{\mathrm{op}}/K_{\mathrm{max}})_{\mathrm{th}\infty} = A_0 + A_1 R + A_2 R^2 + A_3 R^3 \tag{4}$$

with

$$A_0 = (0.875 - 0.34\alpha + 0.05\alpha^2)(\cos K_{\mathrm{th\,max}\infty}/2\sigma_0)^{1/\alpha}$$
$$A_1 = (0.415 - 0.071\alpha)K_{\mathrm{th\,max}\infty}/\sigma_0$$
$$A_2 = 1 - A_0 - A_1 - A_3$$
$$A_3 = 2A_0 + A_1 - 1.$$

The flow stress σ_0 is the average between the uniaxial yield stress and uniaxial ultimate tensile strength of the material: $\sigma_0 = (\sigma_y + \sigma_{\mathrm{uts}})/2$.

The Newman's equation (4) is a function of stress ratio R, stress level $K_{\mathrm{th\,max}\infty}$ and 3-dimensional constraint. The effect of 3-dimensional constraint have been

simulated in a 2-dimensional closure model by using a "constraint" factor α on tensile yielding: that is the material yields when the stress is $\alpha\sigma_y$. The material is assumed to yield in compression when the stress is $-\sigma_y$. The plane stress or plane straian conditions are simulated in the model with $\alpha = 1$ or $\alpha = 3$, respectively.

The specimen used in SKF experiments is thick and fulfils plane strain conditions, and hence $\alpha = 3$ in this case. However, in a practical case, plane strain does not exist at the specimen surface. As a consequence the average plastic constraint factor is much lower than 3. In fact, the crack-opening stresses vary through the thickness of a specimen. Thus, the overall growth rate at low ΔK values may be controlled by a higher constraint factor than that of plane stress. To determine the proper constraint factor, a 3-dimensional analysis would be required. Newman [22] also shows that even for plane strain condition, near threshold stress intensity, the $\alpha = 1$ curve agrees better with the experiments. This is not a surprise because experiments take care of all mentioned contributions to closure, while Newman's model neglects surface roughness, residual stresses and oxide debris. Furthermore, Newman leaves room for speculations on determining factor α. He suggests to take $\alpha = 1$ if one wants curves da/dN vs ΔK to coincide at threshold, and $\alpha = 3$ in order to have overlapping of these curves at ΔK values close to fracture toughness. It turns out that there is not a fixed criterion for determining this factor, it is only certain that $1 < \alpha < 3$.

Newman's curves $(K_{op}/K_{max})_{th\infty}$ vs R in Fig. 5 are designated by NMI and NM3 for $\alpha = 1$ and 3, respectively. It can be seen that no one of these curves can correlate all variants. One cannot choose a single curve which would be suitable for all variants, as Newman claims [24]. It is possible that the discrepancy is due to the fact that Newman's model treats only plasticity induced closure and 2-dimensional case.

The values for threshold effective stress intensity calculated by Newman's model are given in Table 4. It can be seen that they differ for different R values, contradictory to the property of $K_{eff\,th}$ that it is R-independent for any of the α-value. They also differ for different variants, same α and R. In Newman's formulae we assumed that $\sigma_{max}/\sigma_0 = 1/3$, the ratio being same as in our experiments.

Table 4

	$\Delta K_{eff\,th\infty}$						
code	$\alpha = 3$		$\alpha = 1.7$		$\alpha = 1$		our result
	$R = 0.1$	$R = 0.5$	$R = 0.1$	$R = 0.5$	$R = 0.1$	$R = 0.5$	
SA	9.8	6.6	8.3	6.0	6.8	4.6	4.7
TT	7.1	4.9	6.0	4.4	5.0	3.3	3.4
N	3.3	3.6	2.8	3.2	2.3	2.4	3.4
B	6.5	4.6	5.5	4.1	4.5	3.1	3.4
S1	4.5	3.9	3.8	3.5	3.1	2.7	3.4
MA	3.6	3.7	3.1	3.3	2.6	2.5	3.4

The estimated values for $\Delta K_{eff\,th\infty}$ based on experimental results for $\Delta K_{th\infty}$ for long cracks were given in Table 3. Microstructure of soft and hard variants

differ and therefore, even though the effective threshold stress intensity is a material intrinsic property, we chose two different values; 4.6 for the soft SA variant, and the average value 3.4 for hard variants, Table 4. It is evident that these values agree better with the definition of threshold effective stress intensity than the values obtained by using Newman's model with any value of α.

In Fig. 6, which is obtained from Fig.3 and the values from Table 4 by multiplying corresponding points by appropriate factor $\Delta K_{\text{eff th}\infty}/\Delta K_{\text{th}\infty}$, the scattering of long crack data bounded by the curves N, $R = 0.5$ and SA, $R = 0.1$ is evident. It is generally known that by introducing effective stress intensity the band width is reduced. However, Newman's model, which is also based on this, effective stress, concept insignificantly reduces the band width, bounded by dashed lines in Fig. 6 (for $\alpha = 1.7$). From Table 4 it is seen that for $\alpha = 1$, the band is of the similar width, while for $\alpha = 3$ it is even wider although that value of α corresponds to the plane strain situation. In other words, there is not a single value of α such that the curves da/dN vs ΔK would coincide at threshold, contrary to Newman's suggestion [24]. On the other hand, with $\Delta K_{\text{eff th}\infty}$ values calculated the way we did, the band width for hard variants is significantly reduced, being equal to $3.5 - 3.2 = 0.3$, Table 4, Fig. 6.

In general, the Kitagawa-Takahashi diagrams are of the form given in Fig. 7 [16,17]. The sloping lines correspond to $K_{\text{th max}\infty}$ and $K_{\text{eff th max}\infty}$ for long cracks, drawn in log-log scale with the slope 1/2. They intersect the horizontal line corresponding to the fatigue limit (at $N = 5 \times 10^6$) at crack lengths a_0 and a_0', respectively.

Region I is referred to as microstructurally short cracks, namely the crack length is of the order of relevant microstructural unit, for example grain size. Here continuum mechanics assumptions fail.

The long crack behavior is in region III. It can be seen that material initially containing a long crack would fail when K exceeds its threshold value.

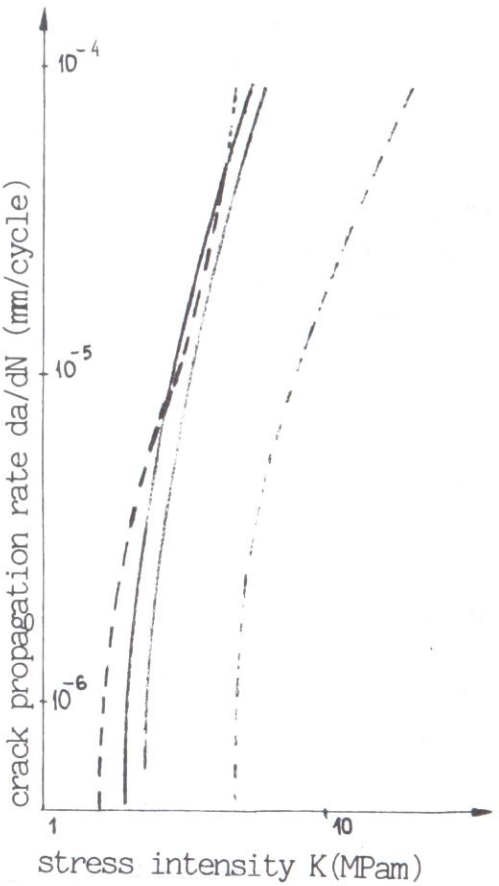

Figure 6

The "anomalous" behavior of cracks which are physically short but several times larger than the microstructural unit, typically 10–15 microstructural units [6,25], is represented by region II. The continuum mechanics limitations are satisfied and elastic-plastic fracture mechanics (EPFM) must be applied. For these physically short cracks the effect of closure is dominant. The significance of the position of the experimental data in this region is that both the S-N prediction and

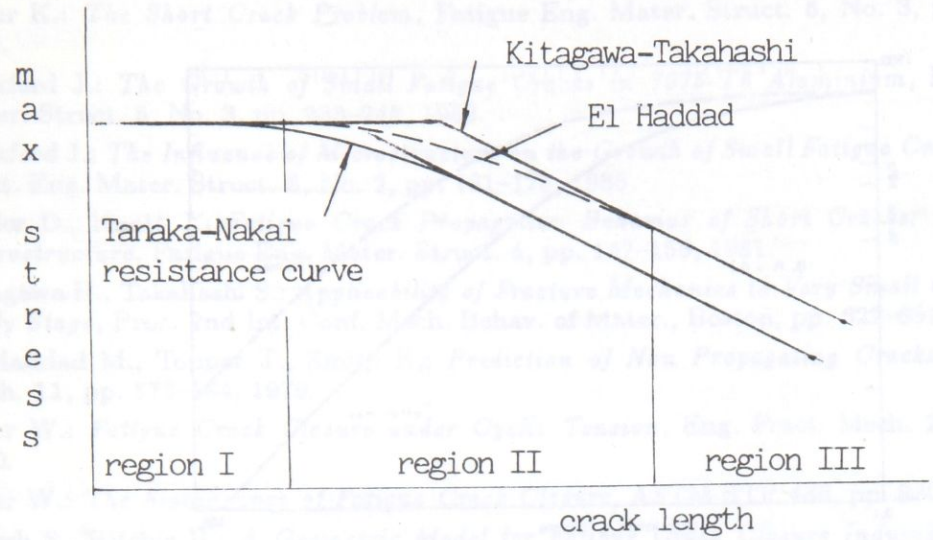

Figure 7

the LEFM prediction of endurance limit are non-conservative.

If the applied stress is larger than the fatigue limit, represented by the resistance curve, then the region I corresponds to stage I, mode II (shear mode) crack propagation. Regions II and III are characterized by stage II, mode I (opening mode) crack propagation for stress levels close to the fatigue limit. However, for very large applied stresses (of the order of yield stress) mode III (tearing mode) crack propagation may occur in stage II for both physically short and long cracks, [26].

The most conservative estimate for non-propagating cracks is obtained by Tanaka and Nakai resistance curves, Fig. 7. Below that curve there is no crack propagation.

Using the experimental data for the endurance limit, threshold stress and threshold effective stress intensities for long cracks, Tables 2,3, the critical crack lengths a_0 and a_0' can be computed from equations (1), (2), and are given in Table 5.

Table 5

		SA	TT	N	B
a_0 (μm)	$R = 0.1$	355	106	3	12
	$R = 0.5$	372	82	7	9
a_0' (μm)	$R = 0.1$	56	17	2	2
	$R = 0.5$	183	40	7	5

Kitagawa-Takahashi diagram for bainitic steel, for example, is in Fig. 8, and similar diagrams are for other heat treated variants.

4. Conclusion. The theoretical treatment of short cracks developed in this work was based on experimental data for long crack propagation. The effective

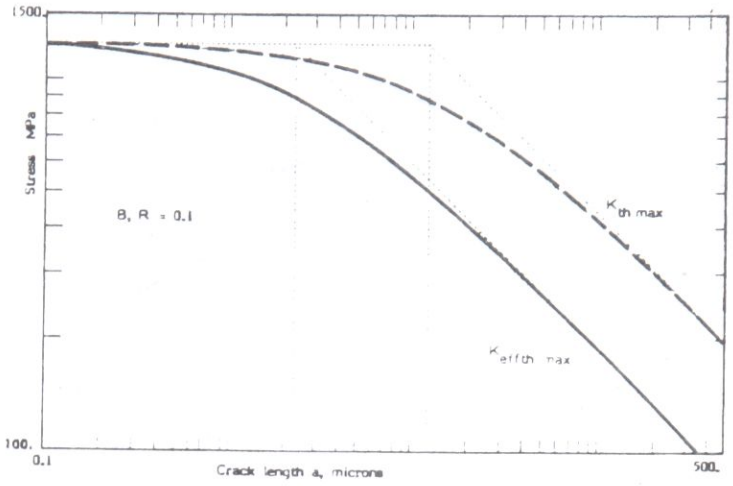

Figure 8

threshold stress intensity values were evaluated by an analytical expression in which the constants were calculated using these experimental data. Unfortunately, the interpolation curves were drawn through only few points. Nevertheless, the results obtained show better correlation between long and short crack propagation than those calculated by using the only existing theory — Newman's model. Moreover, for this particular bearing steel, Newman's model turned out to be inapplicable.

More experimental work to determine the threshold stress intensities for long cracks at high stress ratios is necessary. Even these data would not be enough for verification of the theory developed, since only experiments in which closure is measured can confirm our results and, in general, describe short crack behavior. Unfortunately, the measurement of closure effect is difficult and tedious, although it can be done.

In our theory closure is treated globally, that is contributions due to plasticity, roughness, residual stresses and oxide dobris are included simultaneously. It is our belief that further investigations should be aimed to assessment of each of the contributions separately.

For hardened bearings, the mode I $\Delta K_{th\infty}$ measured on large CT specimen will be the same as the short crack threshold for cracks greater than approximately 20 microns. For soft variants, this critical value is of the order of 400 microns.

Acknowledgment: This work was performed as a part of joint research project of UNIS-Institute, Sarajevo, Yugoslavia and SKF Engineering and Research Centre, Nieuwegein, The Netherlands. The experimental data for long cracks were supplied by SKF-ERC from measurements made at KTH, Stockholm, Sweden. The authors wish to thank the Head of the Physical Metallurgy Department SKF-ERC Mr. J. M. Beswick for his kind support and encouragement to publish the paper.

REFERENCES

[1] Leis B., Hopper A., Ahmad J., Broek D., Kanninen M.: *Critical Review of the Fatigue Growth of Short Cracks*, Eng. Fract. Mech. **23**, No. 5, pp. 883–898, 1986.

[2] Suresh S., Ritchie R.: *Propagation of Short Fatigue Cracks*, Int. Met. Rev. **29**, No. 6, 1984.

[3] Miller K.: *The Short Crack Problem*, Fatigue Eng. Mater. Struct. **5**, No. 3, pp. 223–232, 1982.

[4] Lankford J.: *The Growth of Small Fatigue Cracks in 7075-T6 Aluminium*, Fatigue Eng. Mater. Struct. **5**, No. 3, pp. 233–248, 1982.

[5] Lankford J.: *The Influence of Microstructure on the Growth of Small Fatigue Cracks*, Fatigue Fract. Eng. Mater. Struct. **8**, No. 2, pp. 161–175, 1985.

[6] Taylor D., Knott J.: *Fatigue Crack Propagation Behavior of Short Cracks; the Effect of Microstructure*, Fatigue Eng. Mater. Struct. **4**, pp. 147–155, 1981.

[7] Kitagawa H., Takahashi S.: *Applicability of Fracture Mechanics to Very Small Cracks in the Early Stage*, Proc. 2nd Int. Conf. Mech. Behav. of Mater., Boston, pp. 627–631, 1976.

[8] El Haddad M., Topper T., Smith K.: *Prediction of Non Propagating Cracks*, Eng. Frac. Mech. **11**, pp. 573–584, 1979.

[9] Elber W.: *Fatigue Crack Closure under Cyclic Tension*, Eng. Fract. Mech. **2**, pp. 37–45, 1970.

[10] Elber W.: *The Significance of Fatigue Crack Closure*, ASTM STP 486, pp. 230–242, 1971.

[11] Suresh S., Ritchie R.: *A Geometric Model for Fatigue Crack Closure Induced by Fracture Surface Roughness*, Metall. Trans. A, Vol. **13A**, pp. 1627–1631, 1982.

[12] Tanaka K., Nakai Y.: *Propagation and Non-propagation of Short Fatigue Cracks at a Sharp Notch*, Fatigue Eng. Mater. Struct. **6**, No. 4, pp. 315–327, 1983.

[13] Tanaka K., Akiniwa Y.: *Resistance-Curve Method for Predicting Propagation Thresshold of Short Fatigue Cracks at Notches*, Eng. Fract. Mech. **30**, No. 6, pp. 863–876, 1988.

[14] Beswick J.: *Fracture Mechanics Concept and Applications for Bearing Steels*, Technical Report 8, SKF Engineering and Research Center, Nieuwegein, Holland, 1984.

[15] James M., Knott J.: *An Assessment of Crack Closure and the Extent of the Short Crack Regime in Q1N (HYBO) Steel*, Fatigue Fract. Eng. Mater. Struck. **8**, No. 2, pp. 177–191, 1985.

[16] Kendall J., James M, Knoott J.: *The Behavior of Physically Short Fatigue Cracks in Steels*, The Behavior of Short Fatigue Cracks, Eds. K. Miller and E. R. de los Rios, Mech. Eng. Publs. Ltd., London, pp. 241–258, 1986.

[17] Blom A., et al.: *Short Fatigue Crack Growth Behavior in Al 2024 and Al 7475*, The Behavior of Short Fatigue Cracks, Eds. K. Miller and E. R. de los Rios, Mech. Eng. Publs. Ltd., London, pp. 37–66, 1986.

[18] Blom A., Hadrobletz A., Weiss B.: *Effect of Crack Closure on Near-Threshold Crack Growth Behavior'in a High Strength Al-Alloy up to Ultrasonic Frequencies*, Proc. **ICM4**, Vol. **2**, pp. 755–762, 1983.

[19] Haubaum F., Fine M.: *Short Fatique Crack Growth Behavior in a High Strength Low Alloy Steel*, Scripta Metall. **18**, pp. 1235–1240, 1984.

[20] Kujawski D., Ellyin F.: *A Fatigue Crack Growth Model with Load Ratio Effects*, Eng. Fract. Mech. **28**, No. 4, pp. 367–378, 1987.

[21] Newman Jr. J.: *A Crack Opening Stress Equation for Fatigue Crack Growth*, Int. J. Fract. **24**, 131–135, 1984.

[22] Newman Jr. J.: *A Finite-Element Analysis of Fatigue Crack Closure*, ASTM STP **590**, pp. 281–301, 1976.

[23] Newman Jr. J.: *A Crack-Closure Model for Predicting Fatigue Crack Growth under Aircraft Spectrum Loading*, ASTM STP **748**, pp. 53–84, 1981.

[24] Newman Jr. J.: *A Nonlinear Fracture Mechanics Approach to the Growth of Small Cracks*, Behavior of Short Cracks in Airframe Components, AGARD-CP-328, pp. 6.1–6.26, 1983.

[25] Taylor D.: *Fatigue of Short Cracks: the Limitations of Fracture Mechanics*, The Bahavior of Short Fatigue Cracks, Eds. K. Miller and E. R. de los Rios, Mech. Eng. Publs. Ltd., London, pp. 479–490, 1986.

[26] Brown M.: *Interfaces Between Short, Long, and Non-Propagating Cracks*, The Behavior of Short Fatigue Cracks, Eds. K. Miller and E. R. de los Rios, Mech. Eng. Publs. Ltd., London, pp. 423–439, 1986.

KRITISCHE SPANNUNGSINTESITÄT UND DIE TOLERANZ DER DEFEKTEN DER KURZ SPALTEN IM LAGEREISEN 52100

In der Arbeit sind die Resultaten der Forschung vom Benehmen der kurze Spalten im Lagereisen SAE 52100. Das analytische Model ist entwickelt für das Voraussehen der Vergrösserung der kurzen Spalte. Das Model ist auf der elastoplastischer Mechanik des Bruches und auf dem Konzept der effektiven Spannungsintensität basiert, bzw. auf dem Konzept der Spaltenschliessung. Die Grenzwerte der effektiven Spannungsintesität ist vergleicht mit dem vorher bekommenen beim benutzen des Newmanschen analytischen Model. Die Werte sind ausgenutzt für das Bestimmen der Toleranzdefekten und für das Voraussehen der Spaltenentwicklung basiert auf der Resistenzkurve von Tanaka.

INTENZITETI KRITIČNIH NAPONA I TOLERANCIJE DEFEKATA KRATKIH PUKOTINA U ČELIKU ZA LEŽAJEVE 52100

U radu su dati rezultati istraživanja o ponašanju kratkih pukotina u čeliku za ležajeve SAE 52100. Razvijen je analitički model za predviđanje rasta kratke pukotine. Model je baziran na elasto-plastičnoj mehanici loma i na konceptu efektivnog intenziteta napona, odnosno na konceptu zatvaranja pukotine. Granične vrijednosti efektivnog intenziteta napona su upoređene sa onim dobijenim koristeći Njumanov analitički model. Te vrijednosti su iskorištene za određivanje tolerancije defekata i predviđanje rasta pukotine na osnovu Tanaka rezistentne krive.

Prof. dr Aida Kadić-Galeb
UNIS-Institut
Tršćanska 7
71000 Sarajevo

Prof. dr Hajrudin Pašić
Mašinski fakultet
71000 Sarajevo